Computer Simulation of Amide Bond Formation in Aqueous Solution

S. Chalmet, W. Harb, and M. F. Ruiz-López*

Laboratoire de Chimie théorique, UMR CNRS-UHP No. 7565, Université Henri Poincaré-Nancy I, BP 239, 54506 Vandoeuvre-les-Nancy Cedex, France.

Received: September 18, 2001

We report a theoretical study on ester aminolysis reaction mechanisms in aqueous solution. It is believed, in general, that the formation of a zwitterionic intermediate plays a key role in the aminolysis process whose rate determining step is the formation or breakdown of such an intermediate, depending on pH. However, the reaction mechanism has been object of some recent experimental controversy. We have investigated the model reaction ammonia + formic acid. Stepwise and concerted processes have been studied. Static and dynamic solvent effects have been analyzed by using a dielectric continuum model in the first case and molecular dynamics simulations together with the QM/MM method in the second case. The results show that a zwitterionic structure is always formed in the reaction path although its lifetime appears to be quite dependent on solvent dynamics.

1. Introduction

The amide bond formation mechanism has attracted much attention over the years particularly because of its relevance to understand the synthesis of peptides from amino acids or their esters in prebiotic conditions. The most interesting reaction in this context is the aminolysis of alkyl esters in aqueous solution, which is subjected to general acid−base catalysis. Much experimental work has been reported by Jencks and coworkers,[1−4] supporting a stepwise mechanism with formation of the zwitterionic intermediate $T^{\pm}$ shown in Scheme 1. Such an intermediate may lead to the ionic and neutral forms shown in Scheme 2 through proton transfer. At high pH, formation of the intermediate would be rate-determining, whereas at lower pH, the rate-determining step would be the breakdown to amide. Nevertheless, this reaction mechanism has been the object of some recent controversy. On one hand, isotopic effects studied by Marlier et al.[5] for the hydrazinolysis of methyl formate have led these authors to the conclusion that at pH 10 the rate-determining step of the reaction would be the concerted formation of the anionic tetrahedral intermediate T^{-}. On the other hand, Singleton et al.[6] have given a different interpretation of the results of Marlier et al. based on theoretical calculations. These authors have computed isotope effects for the formation of several hydrated $T^{\pm}$ structures and have reported an explanation for the apparently conflicting mechanistic observations in ester aminolysis.

Theoretically, the mechanism of the uncatalyzed amide bond formation has been investigated by Oie et al.[7] and Jensen et al.,[8] who have shown that stepwise and concerted mechanisms may compete since both involve comparable activation energies. The two mechanisms are summarized in Figure 1. Oie et al.[9] have considered the model reaction of ammonia with formic acid to yield formamide and water at the semiempirical and ab initio levels. According to their results, in the stepwise mechanism, the rate-determining step is the first one. The whole free energy of activation for the stepwise mechanism, i.e., the relative

SCHEME 1

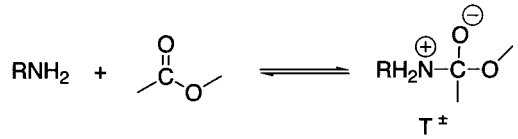

SCHEME 2

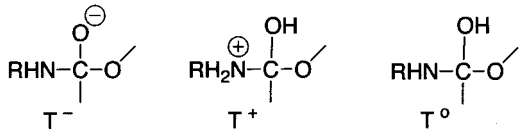

energy of the upper TS with respect to reactants, is $\Delta G^{\ddagger} = 55.3$ kcal/mol at the highest computational level. It is only slightly smaller than the activation free energy for the concerted process, $\Delta G^{\ddagger} = 57.5$ kcal/mol. Similar results have been obtained by Jensen et al.[8] using a higher ab initio level (53.0 and 56.1 kcal/mol respectively). The latter authors performed also a study for the glycine + glycine reaction. The main conclusion was that the model system ammonia + formic acid appears to be a good representative of the dipeptide system with similar geometries and energetics. Oie et al.[9] have also studied an assisted mechanism by a second ammonia molecule showing that there is a catalytic effect that decreases the activation barrier by about 10 kcal/mol for the stepwise mechanism and by about 2 kcal/mol for the concerted one. A related process, the ammonia addition to formaldehyde assisted by water, has been investigated by Williams.[10]

Much more theoretical work has been devoted to the reverse process, i.e., amide hydrolysis, both in gas phase and in water solution. Krug et al.[11] studied the acid and base promoted reaction in gas phase. Antonczak et al.[12,13] described water-assisted mechanisms for neutral and acid promoted reactions in gas phase and in aqueous solution. Dobbs et al.[14] reported reaction enthalpies for neutral amide hydrolysis. Hori et al.[15] made a theoretical study on the influence of leaving groups, including solvent effects. Zheng and Ornstein[16] performed

* Corresponding author. E-mail: Manuel.Ruiz@lctn.uhp-nancy.fr. Tel.: 33 3 83 91 20 50. Fax: 33 3 83 91 25 30. UMR CNRS-UHP No. 7565 is part of the Institut Nancéien de Chimie Moléculaire.

10.1021/jp0135656 CCC: $20.00
Published on Web 11/29/2001

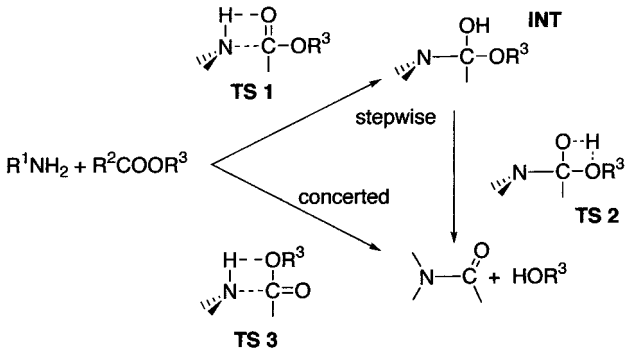

Figure 1. Stepwise and concerted mechanisms proposed in the literature for amide bond formation.

calculations in gas phase and solution for the nucleophilic addition of hydroxide anion to *N*,*N*-dimethyl-acetamide. Kallies and Mitzner[17] modeled the water-assisted hydrolysis in solution comparing the reactivity of methyl formate, formamide and urea. Bakowies and Kollman[18] studied base-catalyzed hydrolysis in aqueous phase using an explicit solvent model and Monte Carlo simulations. Theoretical investigations have also been devoted to the hydrolysis of biologically interesting amides such as β-lactams[19−24] or peptides.[25−27] These works have clarified many aspects of amide hydrolysis mechanisms and have allowed evaluating the activation energies involved. They have underlined, in particular, the considerable role of solvent molecules that may play an active role along the reaction path.

Coming back to amide bond formation mechanisms, the role of the solvent has not been examined in detail yet. However, it is expected to be important considering the possible mediation of charged intermediates. Moreover, the dynamic aspects of the reaction in solution may be fundamental since the lifetime of the complex $T^{\pm}$ appears to be a key factor in the mechanism.[28] In the present work, we examine a few aspects of the problem. Specifically, we consider the reaction mechanism of the uncatalyzed model reaction $NH_3 + HCOOH$ in aqueous solution that according to Jensen et al.[8] is a good representative of dipeptide systems. First, the reaction path is described with the help of density functional theory calculations using a dielectric continuum to model the solvent. Afterward, dynamics aspects are discussed in terms of molecular dynamics simulations of reactive trajectories. In the latter, we use the combined quantum mechanics and molecular mechanics (QM/MM) method described before.[29]

2. Computational Approach

We use density functional theory (DFT) to describe the chemical system, i.e., ammonia and formic acid. The basis set is (621/411/1) for N, C, and O atoms and (41/1) for H as implemented in deMon.[30,31] The gradient-corrected functional of Becke−Perdew[32−34] has been used. This level has been selected as a good compromise between accuracy and computational cost and is close to that employed by previous authors.[13,14,17] Two different solvent models are employed that are described hereafter.

2.1. Continuum Model. We use the self-consistent reaction field (SCRF) model developed in our group.[35−37] The solvent is described by a polarizable continuum medium characterized by its dielectric constant ($\epsilon = 80$ here). The solute−solvent interaction is computed using a multipole moment development and is included into the solute's Hamiltonian. Geometry optimizations and transition state locations are carried out rigorously using a general cavity adapted to the molecular shape. It consists on the surface defined by van der Waals atomic spheres with modified radii (standard Bondi radii multiplied by 1.308). Free energies are obtained with the standard procedures[38] and adding the free energy of solvation. Dispersion and cavitation energies are neglected. Their computation is possible in this model,[39] but their contribution is usually small. Indeed, cavitation and dispersion have different signs and in general similar absolute values so that their contribution tend to vanish. The calculations are carried out with a modified version[40] of SCRFPACK[41] and Gaussian 94.[42]

2.2. Molecular Dynamics Simulations. Molecular dynamics (MD) simulations have been carried out for the chemical system in a box of discrete water molecules. The force field employed is based on the so-called QM/MM method. The chemical system is described quantum mechanically (we employ the DFT level above). The water molecules are described by a molecular mechanics potential (the TIP3P[43] potential is assumed). The quantum solute/classical solvent interaction term contains electrostatic and nonelectrostatic contributions, and therefore, the solute polarization is explicitly taken into account. The Lennard-Jones QM parameters required to calculate the QM/MM van der Waals interactions are those due to Jorgensen and Svenson.[44] The computations are made with the DFMM program implemented in our group.[45]

Since the reaction considered has a high activation barrier (much larger than kT), one cannot use the standard MD approach,[46] the probability to reach the TS from the reactants being too small in the available simulation time. We therefore use a rare-event technique[47,48] that we have implemented in our DFMM program.[29] Accordingly, we define an approximate transition structure (TS) at which MD is started. In principle, the TS obtained in the SCRF approach (TS_{SCRF}) is a good candidate, but we have carried out calculations for a series of structures situated along the SCRF reaction path. Once a trial TS has been selected, it is placed in a box containing TIP3P water molecules, and the whole system is equilibrated with a constrained reaction coordinate. The simulation is continued for a few picoseconds and a number of solute−solvent configurations are saved on disk (separated by at least 500 fs to avoid strong correlations).[49] We then start unconstrained molecular dynamics simulations, integrating the equations of motion backward and forward in time. The initial translational velocities are defined randomly. Technical details may be found elsewhere.[29,49,50]

Molecular dynamics simulations have been performed using a box with sides of 18.8 Å, containing 215 TIP3P water molecules, one quantum ammonia molecule, and one quantum formic acid molecule. Periodic boundary conditions and a cutoff of 9 Å are assumed. Simulations are carried out in the NVE ensemble with a target temperature of 298 K. Other details are given below.

3. Results

As commented above, we only consider here the neutral reaction mechanism. Acid, base, or bifunctional catalysis are expected to be important in this reaction and should be taken into account in order to get a global scheme of the process. They will be considered in forthcoming work. Here, we investigate the main aspects of the mechanism focusing on the role of static and dynamic solvent effects. Due to the computational cost of the present investigation, it has not been possible to extend it to the case of catalyzed reactions. We first present the results obtained using the continuum model that allow us to discuss the solvent effects on the reaction path. Then we

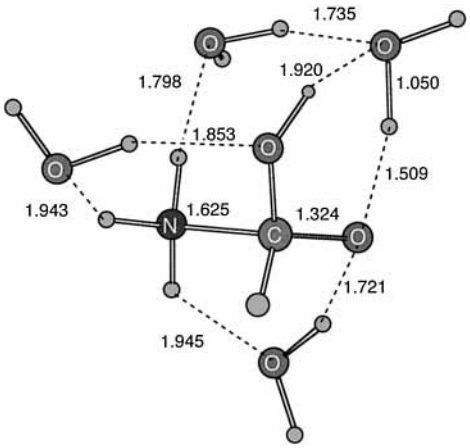

Figure 2. Optimized structure of the tetrahydrated reaction intermediate $T^{\pm}$. Values in Å.

compute reaction trajectories and discuss the dynamic solvent effects using the rare-event MD approach.

3.1. Solvent Effects on Reaction Path. The main solvent effect expected for this reaction, is the stabilization of the intermediate $T^{\pm}$ in aqueous solution. Therefore, special attention has been paid to this point. Geometry optimization of the zwitterion $H_3N^+-CH(OH)O^-$ in gas phase has led to the separated reactants. Previous computations by Singleton et al.[6] for $H_3N^+-C(CH_3)(OH)O^-$ (at a comparable computational level) have shown that the addition of four explicit water molecules stabilizes the intermediate. A similar result has been obtained in our work for $H_3N^+-CH(OH)O^-$ the corresponding optimized geometry being given in Figure 2. We have estimated the activation energy for the dissociation of the zwitterion that is slightly below 4 kcal/mol (we have obtained this value by simply scanning the CN distance and relaxing the system at each step). In the dielectric continuum, full geometry optimization of the zwitterion leads to the separated reactants. The presence of discrete water molecules is therefore necessary to stabilize the structure of such a species through specific hydrogen-bond interactions. For comparison with the results below, we have made a computation of the total energy of the zwitterion in a dielectric continuum, using the optimized geometry in the hydrated cluster above. It is found to lie 17.3 kcal/mol over the separated reactants.

It is now necessary to consider the other relevant structures TS 1, TS 2, TS 3, and INT in Figure 1. They have been optimized in gas phase and in aqueous solution using the continuum model. Intrinsic reaction coordinate (IRC) calculations have been done to verify the structures linked by each TS that correspond to those schematized in Figure 1. The main geometrical parameters are given in Figure 3. Relative energies are given in Table 1.

The reaction enthalpy computed by Dobbs and Dixon[14] for formamide hydrolysis in gas phase at the QCISD level is 0.9 kcal, which is close to our value 1.43 kcal/mol (the sign must be changed for the reverse reaction). Using experimental heats of formation, the reaction enthalpy in the case of the similar ammonia + acetic acid reaction is 0.4 ± 0.9 kcal/mol,[14] which is also consistent with our results. The reaction free energy for the reaction glycilglycine + $H_2O \rightarrow$ glycine + glycine has been estimated[51] to be 6.3 kcal/mol in aqueous solution not far from our value 4.19 kcal/mol. The computed free energies of activation are comparable to previous results carried out in gas phase although the absolute values are a few kcal/mol lower than some ab initio values.[7,8] Our result for TS 3 is very close to that reported at DFT level by Antonczak et al. (44.64 kcal/mol).[13] A discussion on computational level influence has been reported in the latter reference. Stepwise and concerted processes have similar activation energies, as noted before,[7,8] and both may compete. In the stepwise mechanism, the first step is rate-determining. Solvent effects decrease the relative energy (with respect to reactants) for all the species but do not modify the general scheme.

Solvent effects on the geometries are small for the intermediate INT but are significant for the TSs. The asynchronicity of the NH_3 attack to CO in HCOOH (TS3) is substantial and increases in solution, the forming C···N and O···H bonds being shortened and lengthened, respectively, in the solvation process. The asynchronicity of the ammonia molecule attack to either carbonyl (TS 1) or OH (TS 3) appears more clearly when the corresponding IRCs are considered. This is illustrated in Figure 4, where we have plotted the variation of the energy, dipole moment of the system, and bond lengths of the forming bonds along the reaction coordinate relative to TS 1 (similar results are obtained for TS 3). The Figure shows that the C−N bond is practically formed when proton-transfer begins. This occurs at reaction coordinate $R_c = -1.0$, where the CN bond length is 1.605 Å in aqueous solution (1.699 Å in gas phase). In other words, in the first stage of the reaction, the molecules approach each other forming a zwitterionic structure of $T^{\pm}$ type, not sufficiently stabilized by the continuum to be an energy minimum, as commented above. At a sufficiently short CN distance, proton transfer to the oxygen atom proceeds straightforward. Two remarks can be added: (1) the system structure at $R_c = -1.0$ is very close to that obtained for the tetrahydrated zwitterion in Figure 2, and (2) the energy contribution due to proton transfer is approximately half of the activation barrier in solution but it represents only one-third in gas phase. This is an interesting result since as we have noted in the Introduction, experimental studies suggest that the rate-determining step of the reaction is the intermediate formation or the breakdown to amide depending on pH. We have not considered the influence of pH here, but for the neutral process, we therefore predict that formation of the intermediate to be rate determining in gas phase (and probably in nonpolar media) whereas in aqueous solution both "steps" would exhibit similar energy requirements.

As expected, the dipole moment in solution is much larger than that in gas phase all along the reaction path. In both media, the dipole increases initially and exhibits a maximum value before reaching the TS. This substantial electronic reorganization is essentially connected with the decrease of the CN distance. In solution, the curve shows clearly a plateau indicating that the polar structure is stabilized by the solvent. After the maximum, the dipole moment falls down pronouncedly as a consequence of proton transfer. Note that the polarity of TS 1 (and also that of TS 3) is larger than that of the reactants so that the reduction of the activation barrier noted above is not surprising. On the other hand, due to the rapid charge redistribution during the barrier cross characteristic of proton-transfer processes, one may expect dynamic solvent effects to be important. Indeed, solvent relaxation involves molecular reorientations that cannot occur at the same time scale as the reaction. We investigate now this point using the most appropriate molecular dynamics technique.

3.2. Dynamic Solvent Effects. MD calculations have been carried out for the concerted mechanism only (TS 3) since due to the high computational cost it was not possible to study other reaction mechanisms. However, some of the conclusions obtained for the concerted process should also apply for the

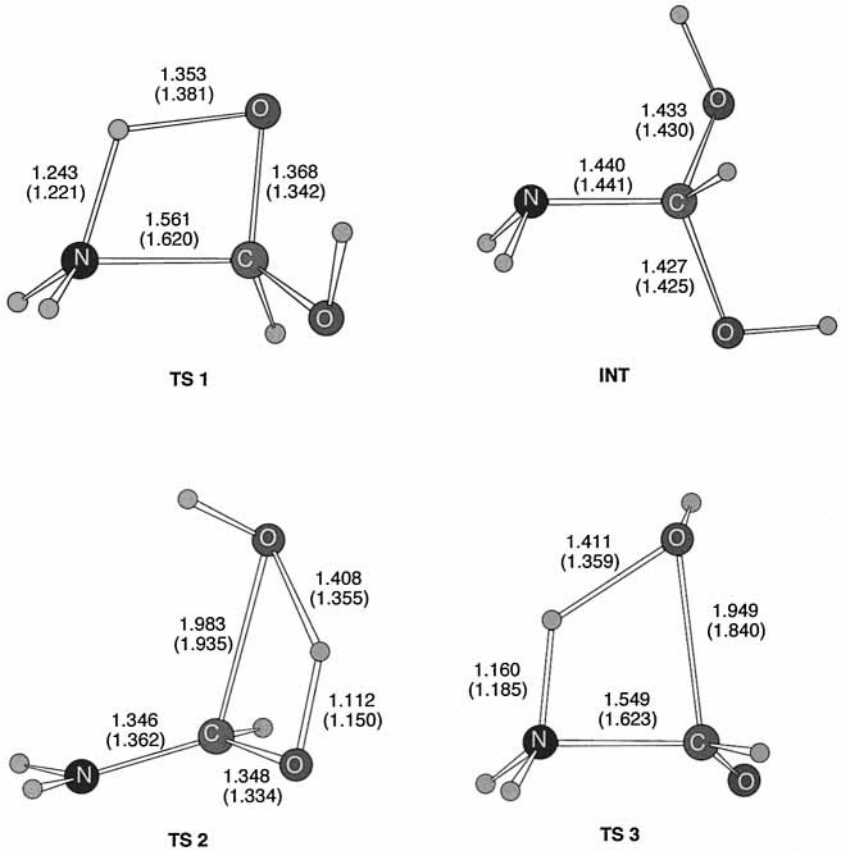

Figure 3. Optimized geometries in aqueous solution and gas phase (in parentheses) for the main structures of the NH_3 + HCOOH reaction (see Figure 1). Values in Å.

TABLE 1: Computed Energies and Free Energies (in kcal/mol) for the Reaction between Ammonia and Formic Acid in Gas Phase and in Aqueous Solution, Using the Dielectric Continuum Model

	gas phase		aqueous solution
	ΔE	ΔG	ΔG
NH_3 + HCOOH	0.0	0.0	0.0
TS 1	33.83	44.32	43.87
INT	4.00	17.46	16.98
TS 2	31.57	41.56	36.78
TS 3	33.60	43.62	41.75
$H_2NCOH + H_2O$	−0.30	−1.43	−4.19

first step of the stepwise mechanism because their characteristics are similar, as noted above.

The starting structure in the simulations was selected by doing some preliminary tests. Basically, the TS is chosen along the SCRF reaction path at $R_c = 0.2$, i.e., slightly after the transition structure found in the continuum model. In fact, simulations starting at $R_c > 0.2$ or $R_c < 0.2$ systematically led to nonreactive trajectories (products to products or reactants to reactants, respectively). The structure at $R_c = 0.2$ ($TS_{DFT/MM}$ hereafter) displays the following distances for the forming and breaking bonds: CN = 1.542 Å, OH = 1.301 Å, NH = 1.237, and CO = 1.960 Å. As shown, $TS_{DFT/MM} \approx TS_{SCRF}$. $TS_{DFT/MM}$ was equilibrated using DFT/MM MD with fixed reaction coordinate, assumed here to be defined by the four distances above. All the other degrees of freedom are unconstrained. After equilibration, the simulation was continued for a few picosenconds and 21 solute−solvent configurations, separated by 500 fs, were saved on disk to start the simulation of reaction trajectories.

Among the computed trajectories, only six led to reactive events (29%). One reactant−reactant trajectory was obtained, whereas the other 14 nonreactive trajectories connected products to products. All the reactive trajectories present the following common feature. Before reaching the TS, a highly polarized structure of $T^{\pm}$ type is formed and proton transfer takes place just before the barrier crossing. This scheme confirms the conclusions of the IRC studies presented above. The difference between the various computed trajectories lies mainly on the lifetime predicted for $T^{\pm}$, that varies from a few femtoseconds to more than 1 ps. We illustrate here these reactive trajectories with two examples that represent extreme situations.

In the first trajectory (t1), the CN distance decreases regularly from reactants to products. It is illustrated in Figure 5, where we have represented the evolution of the distances CN, CO, OH, and NH as a function of time. The proton transfer from N to O (see the NH distance evolution) occurs in the last 25 fs, i.e., once the CN distance is sufficiently small and close to its final value. After the TS, the distances CO and NH increase very quickly, indicating a fast product separation. The OH bond is formed about 25 fs after the barrier crossing. We have represented the evolution of N, O (CO), and O (OH) electronic densities as a function of time in Figure 6 and the system dipole moment variation in Figure 7. During the reaction, the nitrogen atom changes its hybridization type (amine to amide). Accordingly, its negative charge in the reactants decreases from about 0.8 to about 0.4, with fluctuations of about ±0.05. The O (CO) charge increases slightly whereas the O (OH) charge displays a huge increase (from 0.35 to 0.75 in the activation process). The dipole moment exhibits a large increase to reach a maximum (9 D) at about 70 fs before the barrier crossing, corresponding to $T^{\pm}$ formation. The lifetime of this highly polarized conformation is very small, roughly 50 fs. Indeed, about 25 fs before the TS, proton transfer starts, and the dipole

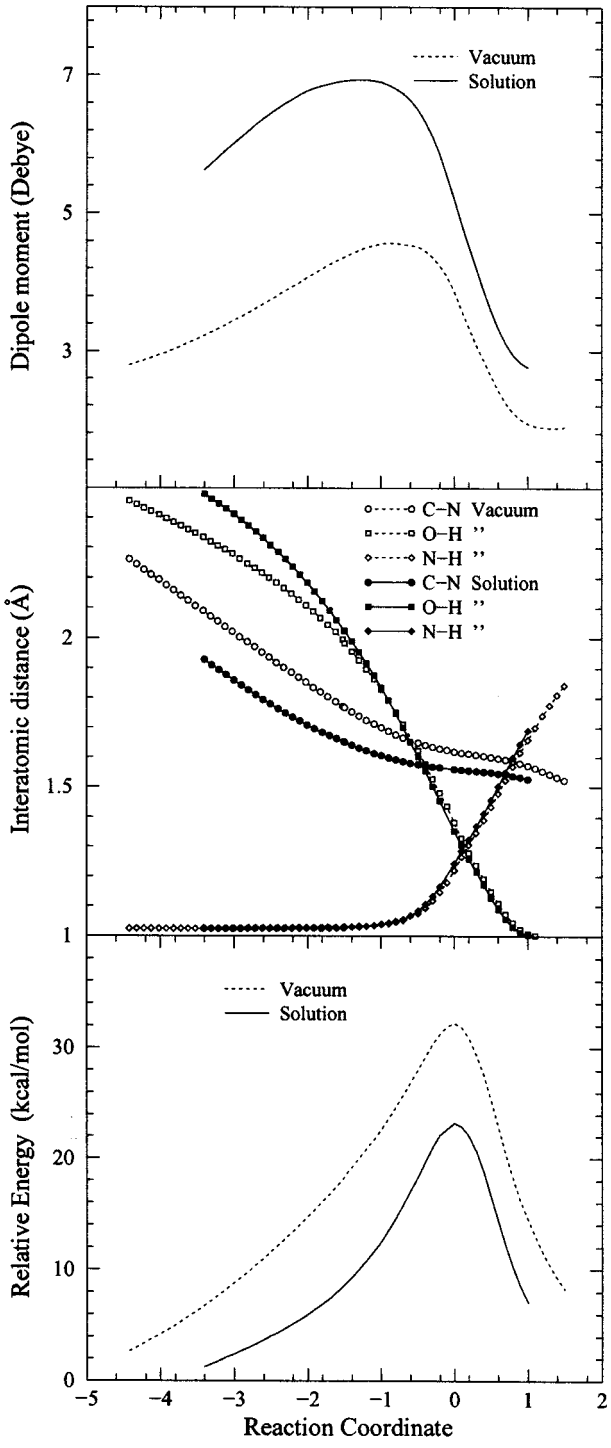

Figure 4. Variation of the energy, dipole moment, and bond lengths of forming bonds along the reaction coordinate relative to TS 1, as given by IRC calculations in gas phase and aqueous solution using the continuum model. The energy is relative to separated reactants and does not include zero-point or thermal corrections.

moment decreases rapidly, reaching a minimum about 25 fs beyond the TS. Then it continues to oscillate in the range 6−7 D.

In the second trajectory (t2), the zwitterionic structure of type $T^{\pm}$ is formed more than 1 ps before reaching the TS. The distances CN, CO, NH, and OH are gathered in Figure 8, the atomic charges in Figure 9, and dipole moment in Figure 10. Before the TS, the C−N distance oscillates between 1.5 and 2.0 Å (average 1.7 Å). The proton transfer from N to O occurs,

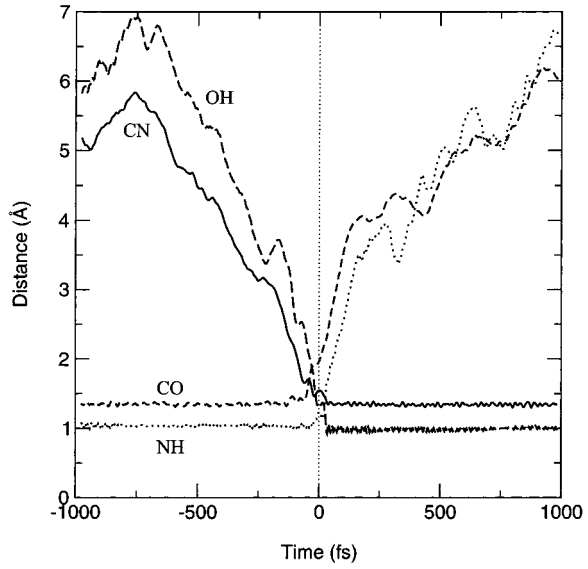

Figure 5. Time evolution of forming and breaking bond distances in trajectory t1. The transition structure TS 3 lies at $t = 0$.

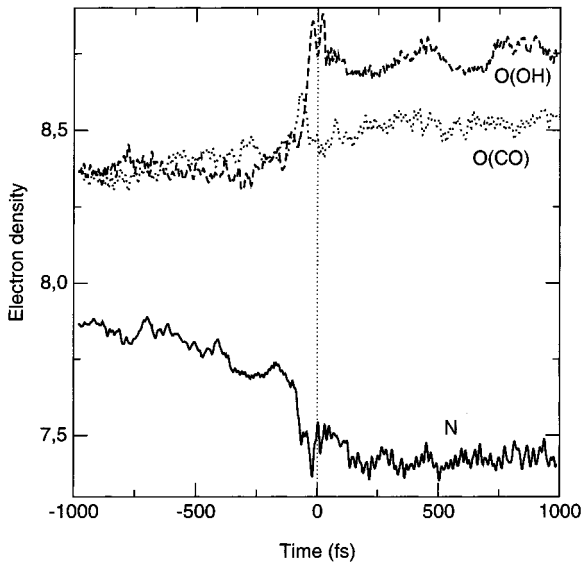

Figure 6. Time evolution of electron densities in trajectory t1 for atoms involved in the forming and breaking bonds.

as in t1, in a very short time. This is accompanied by a fast reorganization of the atomic densities and dipole moment, as shown in the corresponding figures. The dipole moment undergoes a pronounced decrease starting 25 fs before the TS and ending 25 fs after.

The lifetime of the $T^{\pm}$-like structure appears to be quite dependent on solvent dynamics. In turn, the stabilization of $T^{\pm}$ affects the dynamics and energetics of the final part of the activation process, basically defined by proton transfer. For a very fast process occurring in water, one may assume a frozen environment, as shown in previous simulations for proton transfer with a similar DFT/MM technique.[52] On the other hand, the reaction field "felt" by the proton during the barrier crossing depends on the trajectory type. In t2, this reaction field should be rather intense, corresponding to an equilibrated solvent around a zwitterion. In t1, instead, the solvent has not much time to reorganize itself around the short-lived zwitterion, and the reaction field should be smaller than in t2. Indeed, at the TS, the calculated absolute value of the electric field created by solvent molecules at the center of mass of the solute is 0.0195

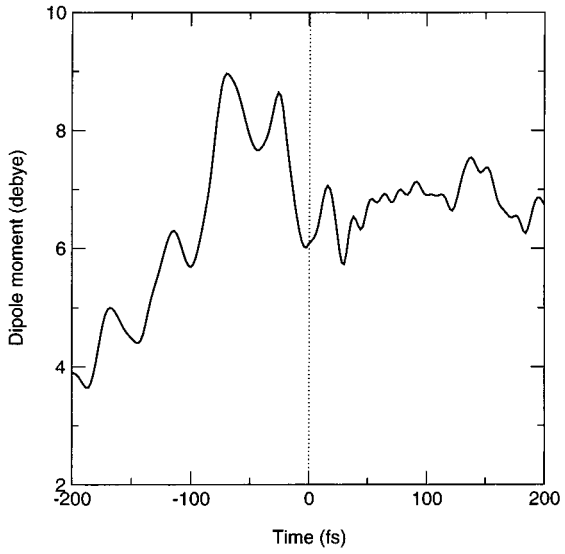

Figure 7. Time evolution of dipole moment in trajectory t1.

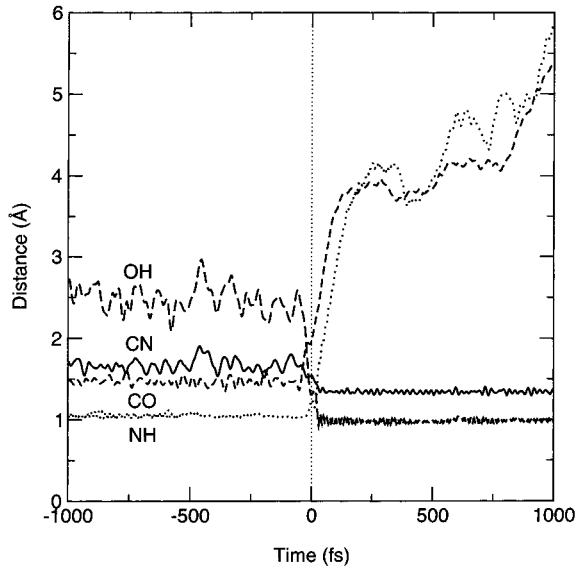

Figure 8. Time evolution of forming and breaking bond distances in trajectory t2. The transition structure TS 3 lies at $t = 0$.

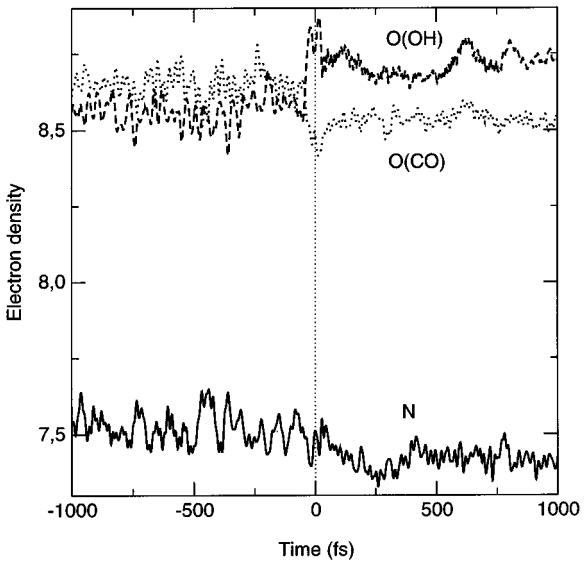

Figure 9. Time evolution of electron densities in trajectory t2 for atoms involved in the forming and breaking bonds.

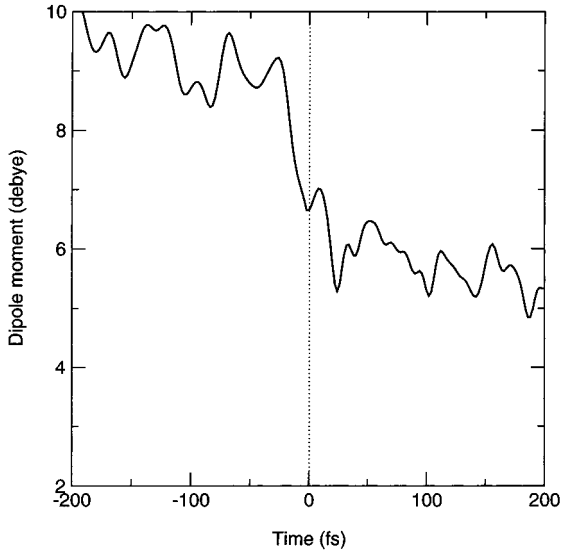

Figure 10. Time evolution of dipole moment in trajectory t2.

au in t1 and 0.0225 au in t2. Proton-transfer involves dipole moment diminution so that the process is favored in a less polarized solvent, i.e., in t1. The potential energy $E_{QM} + E_{QM/MM}$ is shown in Figure 11 and illustrates this point. In t1, the TS is about 25 kcal/mol above the reactants, whereas in t2 it is 35 kcal/mol above them.

To further analyze the role of solvation, we have calculated the number of water molecules participating to hydrogen-bonds with the carbonyl oxygen atom along the reaction trajectories.This is an interesting quantity since it gives an indication of the solute−solvent interaction strength. The average value for reactive and nonreactive trajectories as a function of time is plotted in Figure 12. As shown, the number of water molecules bonded to O(CO) is larger in reactive trajectories. In particular, at the TS, the carbonyl group forms one H-bond in nonreactive trajectories whereas it forms two H-bonds in the reactive ones. Thus, a larger solvation of the carbonyl group is a favoring reaction factor. Or in other words, the probability for a trajectory reaching the TS to proceed toward the products increases with increasing H-bonding on the carbonyl group. Such an effect may be related to acid catalysis in which the protonation of the carbonyl oxygen atom produces a substantial energy decrease.[11,12] Obviously, the effect of hydrogen bonds is smaller but as shown in Table 1, the activation barrier is decreased by the effect of hydration.

4. Conclusion

These computations have allowed us to discuss solvent effects on the reaction of ammonia with formic acid to yield formamide and water in aqueous solution as a model for ester aminolysis. Particular attention has been paid to the role of the zwitterionic species $T^{\pm}$ that has been proposed in the literature to be a key intermediate. Computations with the continuum model do not predict a stable zwitterionic intermediate, whereas a local energy minimum is found by explicit consideration of four solvent water molecules. The stability of such an intermediate is however small, dissociating into reactants easily. We estimate it to lie 17.3 kcal/mol above the separated reactants in aqueous solution.

The stepwise and concerted mechanisms previously described in the literature for the gas phase reaction have been studied in aqueous solution. Though solvent effects modify substantially the energy profile as well as the molecular properties along the

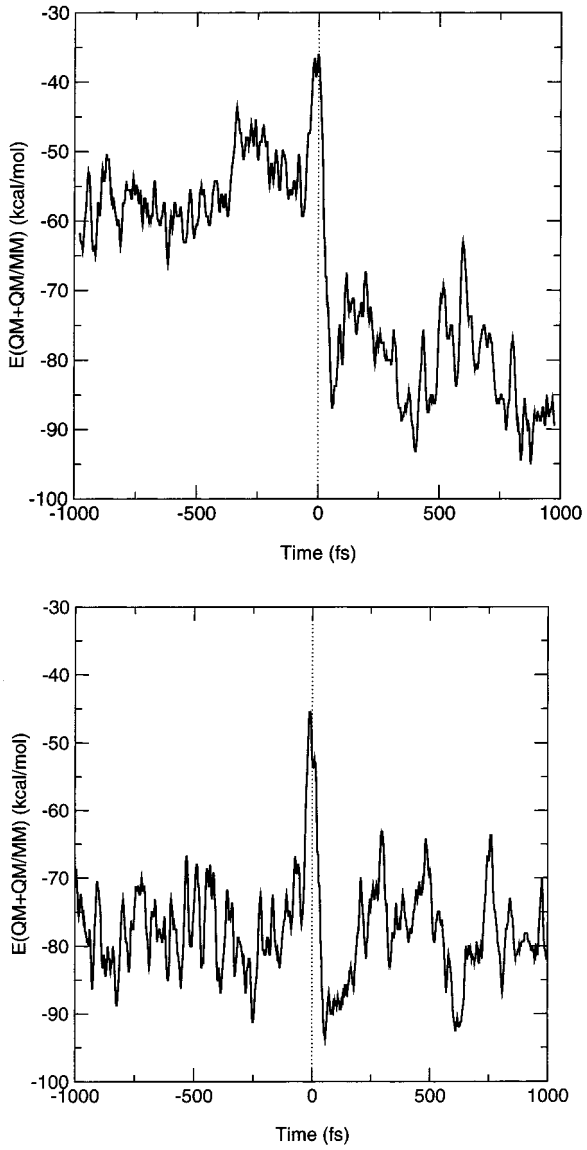

Figure 11. Time evolution of potential energy ($E_{QM} + E_{QM/MM}$) along the trajectories t1 (top) and t2 (bottom).

reaction path, they are not quite large on activation energies. Our computed activation barriers suggest that stepwise and concerted mechanism may compete in water. Both present activation barrier to addition a little larger than 40 kcal/mol.

The analysis of the reaction path has been made using the intrinsic reaction coordinate method. The calculations have shown that $T^{\pm}$-like structures are formed at the beginning of the ester aminolysis path, both in stepwise and concerted mechanisms. When the CN distance attains 1.6−1.7 Å, proton transfer from N to O (CO or OH) takes place. The crossing of the activation barrier is basically done at constant CN distance. In aqueous solution, formation of the intermediate and proton transfer require similar energies, whereas gas-phase calculations predict formation of the intermediate to be much more energy demanding.

Molecular dynamics simulations using the combined DFT/MM method confirm the conclusions reached with the continuum model and have allowed us to estimate the characteristic time scale for the process. Clearly, a $T^{\pm}$-like structure is always found in the simulated trajectories. However, the corresponding lifetime varies from a few femtoseconds to more than 1 ps, depending on initial conditions. The final proton transfer occurs,

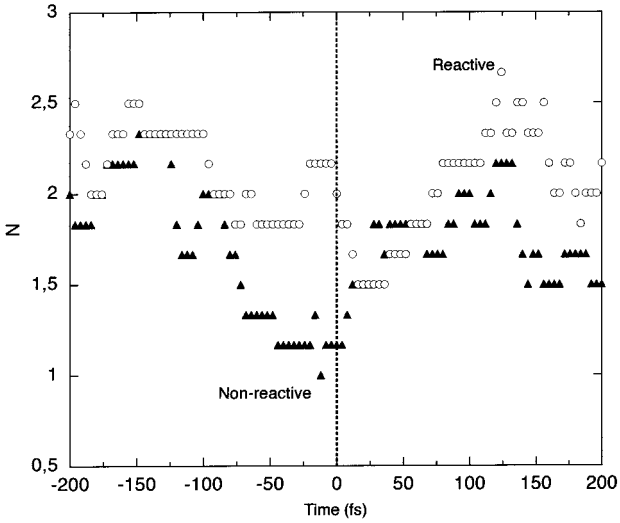

Figure 12. Average number of hydrogen bonds of the carbonyl oxygen atom with water molecules in reactive (circles) and nonreactive trajectories (triangles).

as usual, in a very short time, about 50 fs. The fast change of system polarity accompanying the proton movement prevents full solvent relaxation during the barrier crossing and accordingly nonequilibrium effects are observed. A consequence of these dynamic solvent effects is that many trajectories (roughly 70%) are nonreactive, which should lower the transmission coefficient of the reaction quite significantly.

In the present work, we have used a rare event strategy for the simulation of chemical processes in solution with combined QM/MM methods. Clearly, the most delicate point is the need to define an approximate structure of the TS in solution. This becomes possible with the help of approximate solvent models, such as the continuum one, but is not quite satisfying in the sense that some mechanistic hypothesis are required before making the simulations. Besides, the sampling of the TS region is inevitably oversimplified. Overcoming such approximations is not trivial and remains a major challenge in chemical modeling.

Acknowledgment. The authors thank the CINES (Montpellier, France) for computational facilities (Project No. lct2550).

Supporting Information Available: Energy and Cartesian coordinates of optimized structures (tetrahydrated zwitterion, INT, TS 1, TS 2, and TS 3). Results in gas phase and aqueous solution. This material is available free of charge via the Internet at http://pubs.acs.org.

References and Notes

(1) Gresser, M. J.; Jencks, W. P. *J. Am. Chem. Soc.* **1977**, *99*, 6970.
(2) Yang, C. C.; Jencks, W. P. *J. Am. Chem. Soc.* **1988**, *110*, 2972.
(3) Cox, M. M.; Jencks, W. P. *J. Am. Chem. Soc.* **1981**, *103*, 572, 580.
(4) Satterthwait, A. C.; Jencks, W. P. *J. Am. Chem. Soc.* **1974**, *96*, 7031.
(5) Marlier, J. F.; Haptonstall, B. A.; Johnson, A. J.; Sacksteder, K. A. *J. Am. Chem. Soc.* **1997**, *119*, 8838.
(6) Singleton, D. A.; Merrigan, S. R. *J. Am. Chem. Soc.* **2000**, *122*, 11035.
(7) Oie, T.; Loew, G. H.; Burt, S. K.; Binkley, J. S.; MacElroy, R. D. *J. Am. Chem. Soc.* **1982**, *104*, 6169.
(8) Jensen, J. H.; Baldridge, K. K.; Gordon, M. S. *J. Phys. Chem.* **1992**, *96*, 8340.
(9) Oie, T.; Loew, G. H.; Burt, S. K.; MacElroy, R. D. *J. Am. Chem. Soc.* **1983**, *105*, 2221.

(10) Williams, I. H. *J. Am. Chem. Soc.* **1987**, *109*, 6299.
(11) Krug, J. P.; Popelier, P. L. A.; Bader, R. F. W. *J. Phys. Chem.* **1992**, *96*, 7604.
(12) Antonczak, S.; Ruiz-López, M. F.; Rivail, J. L. *J. Am. Chem. Soc.* **1994**, *116*, 3912.
(13) Antonczak, S.; Ruiz-López, M. F.; Rivail, J. L. *J. Mol. Model.* **1997**, *3*, 434.
(14) Dobbs, K. D.; Dixon, D. A. *J. Phys. Chem.* **1996**, *100*, 3965.
(15) Hori, K.; Kamimura, A.; Ando, K.; Mizumura, M.; Ihara, Y. *Tetrahedron* **1997**, *53*, 4317.
(16) Zheng, Y.-J.; Ornstein, R. L. *J. Mol. Struct. (THEOCHEM)* **1998**, *429*, 41.
(17) Kallies, B.; Mitzner, R. *J. Mol. Mod.* **1998**, *4*, 183.
(18) Bakowies, D.; Kollman, P. A. *J. Am. Chem. Soc.* **1999**, *121*, 5712.
(19) Petrongolo, C.; Pescatori, E.; Ranghino, G.; Scordamaglia, R. *Chem. Phys.* **1980**, *45*, 291.
(20) Petrongolo, C.; Ranghino, G. *Theoret. Chim. Acta* **1980**, *54*, 239.
(21) Petrongolo, C.; Ranghino, G.; Scordamaglia, R. *Chem. Phys.* **1980**, *45*, 279.
(22) Frau, J.; Donoso, J.; Muñoz, F.; García Blanco, F. *J. Comp. Chem.* **1991**, *13*, 681.
(23) Rivail, J.-L.; Loos, M.; Théry, V. In *Trends in Ecological Physical Chemistry*; Bonati, L., Cosentino, U., Lasagni, M., Moro, G., Pitea, D., Schiraldi, A., Eds.; Elsevier: Amsterdam, 1993; pp 17−26.
(24) Pitarch, J.; Ruiz-López, M. F.; Silla, E.; Pascual-Ahuir, J. L.; Tuñón, I. *J. Am. Chem. Soc.* **1998**, *120*, 2146.
(25) Alex, A.; Clark, T. *J. Comp. Chem.* **1992**, *13*, 704.
(26) Antonczak, S.; Monard, G.; Ruiz-López, M. F.; Rivail, J.-L. *J. Am. Chem. Soc.* **1998**, *120*, 8825.
(27) Antonczak, S.; Monard, G.; Ruiz-López, M. F.; Rivail, J.-L. *J. Mol. Mod.* **2000**, *6*, 527.
(28) Jencks, W. P. *Chem. Rev.* **1972**, *72*, 705.
(29) Strnad, M.; Martins-Costa, M. T. C.; Millot, C.; Tuñón, I.; Ruiz-López, M. F.; Rivail, J. L. *J. Chem. Phys.* **1997**, *106*, 3643.
(30) St-Amant, A.; Salahub, D. *Chem. Phys. Lett.* **1990**, *169*, 387.
(31) Salahub, D. R.; Fournier, R.; Mlynarski, P.; Papai, I.; Amant, A. S.; Ushio, J. In *Theory and Applications of Density Functional Approaches to Chemistry*; Labanowski, J., Andzelm, J., Eds.; Springer: Berlin, 1991.
(32) Becke, A. D. *Phys. Rev. A* **1988**, *38*, 3098.
(33) Perdew, J. P. *Phys. Rev. B* **1986**, *33*, 8822.
(34) Perdew, J. P. *Phys. Rev.* **1986**, *B34*, 7406.
(35) Rivail, J. L.; Rinaldi, D. *Chem. Phys.* **1976**, *18*, 233.
(36) Rinaldi, D.; Ruiz-Lopez, M. F.; Rivail, J. L. *J. Chem. Phys.* **1983**, *78*, 834.
(37) Dillet, V.; Rinaldi, D.; Rivail, J. L. *J. Phys. Chem.* **1994**, *98*, 5034.
(38) Hehre, W. J.; Radom, L.; Schleyer, P. v. R.; Pople, J. A. *Ab Initio Molecular Orbital Theory*; Wiley: New York, 1986.
(39) Tuñón, I.; Bertrán, J.; Ruiz-López, M. F.; Rinaldi, D. *J. Comput. Chem.* **1996**, *17*, 148.
(40) Rinaldi, D. Unpublished version adapted to Gaussian 98.
(41) Rinaldi, D.; Pappalardo, R. R. *SCRFPACK*; Quantum Chemistry Program Exchange: Bloomington, IN, 1992.
(42) Frisch, M. J.; Schegel, G. W. T. H. B.; Gill, P. M. W.; Johnson, B. G.; Robb, M. A.; Cheseman, J. R.; Keith, T. A.; Petersson, G. A.; Montgomery, J. A.; Raghavachari, K.; Al-Laham, M. A.; Zakrzeski, V. G.; Ortiz, J. V.; Foresman, J. B.; Ciolowski, J.; Stefanov, B. B.; Nanayakkara, A.; Challacombe, M.; Peng, C. Y.; Ayala, P. Y.; Chen, W.; Wong, M. W.; Andrés, J. L.; Reploge, E. S.; Gomperts, R.; Martin, R. L.; Fox, D. J.; Binkley, J. S.; Defrees, J.; Baker, D. J.; Stewart, J. P.; Head-Gordon, M.; Gonzalez, C.; Pople, J. A. *Gaussian98*; Gaussian, Inc.: Pittsburgh, PA, 1995.
(43) Jorgensen, W. L.; Chandrashekar, J.; Madura, J. D.; Impey, W. R.; Klein, M. L. *J. Chem. Phys.* **1983**, *79*, 926.
(44) Jorgensen, W. L.; Svenson, C. J. *J. Am. Chem. Soc.* **1985**, *107*, 569.
(45) Tuñón, I.; Costa, M. T. C.; Millot, C.; Ruiz-López, M. F. *J. Mol. Mod.* **1995**, *1*, 196.
(46) Whitnell, R. M.; Wilson, K. R. In *Reviews in Computational Chemistry*; Lipkowitz, K. B., Boyd, D. B., Eds.; UCH Publishers, Inc.: New York, 1993; pp 67−148.
(47) Keck, J. C. *Faraday Discuss. Chem. Soc.* **1962**, *33*, 173.
(48) Anderson, J. B. *J. Chem. Phys.* **1973**, *58*, 4684.
(49) Gertner, B. J.; Whitnell, R. M.; Wilson, K. R.; Hynes, J. T. *J. Am. Chem. Soc.* **1991**, *113*, 74.
(50) Chalmet, S.; Thesis, Université Henri Poincaré, Nancy, 2000.
(51) Martin, R. B. *Biopolymers* **1998**, *45*, 351−353.
(52) Tuñón, I.; Costa, M. T. C.; Millot, C.; Ruiz-López, M. F.; Rivail, J. L. *J. Comp. Chem.* **1996**, *17*, 148.